Closed-form Stereo Image Rectification

Changming Sun
CSIRO Mathematics, Informatics and Statistics
Locked Bag 17, North Ryde, NSW 1670, Australia
changming.sun@csiro.au

ABSTRACT

Stereo image rectification transforms a pair of images into a new pair such that the epipolar lines in the transformed images have the same direction as the image rows and matching epipolar lines in different images have the same row index to enable an efficient and reliable dense stereo matching. In this paper we propose a *first closed-form* algorithm to automatically rectify stereo images just using the fundamental matrix. The algorithm involves only direct and purely geometric transformation processes. There is no iterative or optimization processes for the rectification parameter estimation in our method. Real images have been used for testing purposes, and convincing results have been obtained from our algorithm. Comparison with the state-of-the-art method shows that our method produces better rectification results.

Categories and Subject Descriptors

I.2.10 [**Vision and Scene Understanding**]: 3D/stereo scene analysis; I.4.8 [**Scene Analysis**]: Stereo

General Terms

Algorithms

Keywords

Stereo image rectification, Fundamental matrix, Epipolar lines, Epipoles, Keystone effect.

1. INTRODUCTION

Stereo image rectification is important in the analysis of three dimensional scenes. The rectification process transforms the input images into new ones where epipolar lines are parallel to the x- axis and matching epipolar lines from different images have the same row index. This process removes the vertical disparities between matching points in the original left and right images. The rectified images should be positioned on the same plane and parallel to the line connecting the camera centers. The rectification process should introduce minimal distortions for the rectified images. For stereo matching, image rectification can increase both the reliability and the speed of disparity estimation. This is because in the rectified images, the relative rotation between the original images has been removed and the disparity search happens only along the image horizontal scanlines. This rectification is also useful for human viewing of stereoscopic images to reduce vertical parallax which often causes eyestrain.

The rectification process usually requires certain camera calibration parameters or weakly calibrated (uncalibrated) epipolar geometries of the image pair and most algorithms require the initial feature matching points as a part of the inputs. Some algorithms obtain the rectification matrix just from the image matching points.

Ayache and Hansen presented a technique for calibrating and rectifying a pair or triplet of images [1]. In their case, a camera matrix needs to be estimated. Jawed et al. presented a hardware implementation for real time rectification using FPGA [8]. Fusiello et al. presented a compact algorithm for rectifying calibrated stereo images [4]. All these rectification algorithms only work for calibrated cameras where camera parameters are known.

There is also a large number of algorithms for uncalibrated camera cases. Pollefeys et al. proposed a simple and efficient rectification method for general two view stereo images by reparameterizing the image with polar coordinates around the epipoles [14]. A similar approach is described in [2]. These two methods used a direct sampling approach based on the epipolar geometry. A method on the rectification of stereo images onto cylindrical surfaces was given in [16].

Hartley gave a mathematical basis and a practical algorithm for the rectification of stereo images from widely different viewpoints [6]. Oram presented a similar method for rectification for any epipolar geometry [13]. All of the above algorithms require the fundamental matrix and the accompanying matching points information.

Isgrò and Trucco proposed a projective rectification method which uses the matching points to estimate the rectification matrices directly without the use of epipolar geometry [7]. Fusiello and Irsara proposed a quasi-Euclidean rectification method which minimizes a rectification error [3]. Kumar et al. used a similar approach to obtain the rectification matrices directly from image matching points while considering the different zoom factors of the two images [9].

Loop and Zhang proposed a technique for computing rectification homographies for stereo vision using the fundamen-

IVCNZ '2012, November 26-28 2012, Dunedin, New Zealand

tal matrix between images together with all the points in the images to minimize image distortion [10]. Robert et al. described a method for rectification considering the minimization of image distortion by preserving orthogonality and the newly filled areas [15]. A similar approach is used in [5] for obtaining rectifying transformations that minimize resampling effects. Monasse et al. proposed a three-step image rectification method which involves optimizing one parameter [12]. Mallon and Whelan used fundamental matrix and regularly sampled points in the images for rectification [11]. All of these methods use the fundamental matrix and also involve iterative or optimization process for rectification parameters estimation.

In this paper, we propose a first closed-form algorithm for automatically rectifying two uncalibrated images only using the fundamental matrix and no iterative parameter optimization step is involved. All the steps that we used only involve direct geometric transformation.

2. RECTIFYING UNCALIBRATED IMAGES

Our rectification process only requires the fundamental matrix that can be obtained from matching points between two images or from any other methods.

2.1 Move Epipoles to Infinity

Given the epipolar geometry defined by the fundamental matrix $\mathbf{F}_{12}$ between two images, a pair of epipoles $\mathbf{e}_{12}$ and $\mathbf{e}_{21}$ in these two images can be obtained by solving $\mathbf{F}_{12}\mathbf{e}_{12} = \mathbf{0}$ and $\mathbf{F}_{12}^T\mathbf{e}_{21} = \mathbf{0}$ using a singular value decomposition method, and then scaling the epipoles so that the third elements are equal to 1. The image rectification process is to initially transform the input images such that the epipoles in the transformed images are at infinity on the x- axis. In the usual case of left and right stereo image arrangement, the epipoles of the transformed images are at the infinity point $(1, 0, 0)^T$.

One needs to find the mapping functions which will transform the two epipoles $\mathbf{e}_{12}$ and $\mathbf{e}_{21}$ in the two original images into the infinity point $(1, 0, 0)^T$ in the transformed images. In order to reduce image distortions, image transformations need to be as rigid as possible. In the following paragraph, we will describe the algorithm steps for transforming the epipoles into infinity. This transformation steps have been used in several articles [6, 17].

Assuming that the image center is at $(u, v, 1)^T$, one can use the following transformation to shift the image coordinate system to the image center:

$$\mathbf{T} = \begin{pmatrix} 1 & 0 & -u \\ 0 & 1 & -v \\ 0 & 0 & 1 \end{pmatrix}. \quad (1)$$

Then the image can be rotated such that the epipole after translation $\mathbf{e}'_{12} = \mathbf{T}\,\mathbf{e}_{12} = (e'_{12}[0], e'_{12}[1], 1)^T$ is further moved onto the x- axis. This rotation transformation takes the form of

$$\mathbf{R}_1 = \begin{pmatrix} \cos\theta_1 & \sin\theta_1 & 0 \\ -\sin\theta_1 & \cos\theta_1 & 0 \\ 0 & 0 & 1 \end{pmatrix} \quad (2)$$

where $\theta_1 = \arctan(e'_{12}[1]/e'_{12}[0])$. The next step will be to project the epipole position to infinity. This transformation can be achieved using the following matrix:

$$\mathbf{K}_1 = \begin{pmatrix} 1 & 0 & 0 \\ 0 & 1 & 0 \\ -1/k_1 & 0 & 1 \end{pmatrix} \quad (3)$$

where $k_1 = e''_{12}[0]$ with $\mathbf{e}''_{12} = \mathbf{R}_1\,\mathbf{e}'_{12}$. The combined transformation matrix is:

$$\mathbf{P}_1 = \mathbf{K}_1\mathbf{R}_1\mathbf{T}. \quad (4)$$

This transformation will have the effect of projecting the epipole $\mathbf{e}_{12}$ to infinity on the x- axis. Note that the values of θ_1 and k_1 are obtained from the immediate previous transformation operations. A similar transformation for the right image which maps the epipole $\mathbf{e}_{21}$ to infinity on the x- axis can be obtained with $\mathbf{P}_2 = \mathbf{K}_2\mathbf{R}_2\mathbf{T}$. The corresponding values θ_2 and k_2 for $\mathbf{R}_2$ and $\mathbf{K}_2$ for the right image are obtained in a similar way as θ_1 and k_1 for the left image.

2.2 Aligning Matching Epipolar Lines

After moving the epipoles of the two images to infinity by applying $\mathbf{P}_1$ and $\mathbf{P}_2$, the epipolar lines in the two transformed images become parallel to the horizontal scanline. However, the matching epipolar lines from the left and right images usually do not lie on the same scanline. In this section we present our new method for aligning matching horizontal epipolar lines from the two images so that they will have the same y value.

Three pairs of matching epipolar lines from the left and right images are needed for our alignment purpose. These three pairs of matching epipolar lines can be obtained by firstly selecting three points on a vertical line passing through the image center in the left image with the same spacing. The middle point can be the center of the image, and the other two points are one above and one below the center point. The spacing for these points can be arbitrary. Then epipolar lines passing through these three points in the left image can be calculated using the fundamental matrix. The three matching epipolar lines in the right image can also be obtained. These three pairs of matching epipolar lines will all be horizontal after the $\mathbf{P}_1$ and $\mathbf{P}_2$ transformations. The middle epipolar line in the left image goes through the image center. In order to make the matching middle epipolar lines have the same y value, we first align the middle horizontal epipolar lines between the left and right images by shifting the right image vertically with

$$\mathbf{T}_v = \begin{pmatrix} 1 & 0 & 0 \\ 0 & 1 & -v_m \\ 0 & 0 & 1 \end{pmatrix} \quad (5)$$

where v_m is the y difference between the two horizontal middle matching epipolar lines.

Next we need to find the transformation for aligning the remaining two matching epipolar lines. Figure 1 illustrates the cross sections of the two transformed images, perpendicular to the epipolar lines and going through the image center. The x- axis of the epipolar lines is perpendicular to the page. The locations of the three epipolar lines on image plane AMD are shown by the three small black squares, while the locations of the matching epipolar lines on image plane BFE are given by the three small dots which are to be transformed to the locations at A, M, and D. H_1, H_2, G_1, and G_2 are the y coordinates of points A, D, B, and E, respectively. The y coordinates of F and M are now zero after the $\mathbf{T}_v$ shift for the right image.

The transformation matrix for alignment will take a form of a projection matrix. It just transforms one point loca-

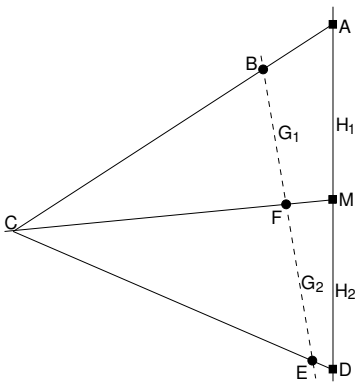

Figure 1: Illustration for aligning matching epipolar lines. Points A, M, D and B, F, E are the y locations of the horizontal epipolar lines. Point C is the camera center. The x- axis of the epipolar lines is perpendicular to the page.

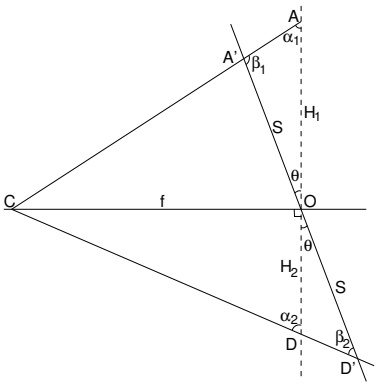

Figure 2: Illustration for keystone effect correction.

tion to another for the matching epipolar lines. Scaling is also necessary in the matrix. Here is the form for aligning epipolar lines from B to A and from E to D:

$$\mathbf{A}_2 = \begin{pmatrix} 1 & 0 & 0 \\ 0 & w_y & 0 \\ 0 & k'_y & 1 \end{pmatrix} \tag{6}$$

where w_y and k'_y will be obtained using the location information of the matching epipolar lines. To transform point B with $\mathbf{A}_2$, we have

$$\begin{pmatrix} 1 & 0 & 0 \\ 0 & w_y & 0 \\ 0 & k'_y & 1 \end{pmatrix} \begin{pmatrix} 0 \\ G_1 \\ 1 \end{pmatrix} = \begin{pmatrix} 0 \\ w_y G_1 \\ k'_y G_1 + 1 \end{pmatrix} \sim \begin{pmatrix} 0 \\ \frac{w_y G_1}{k'_y G_1 + 1} \\ 1 \end{pmatrix} \tag{7}$$

This point matches $(0, H_1, 1)^T$. Therefore, we can have

$$\frac{w_y G_1}{k'_y G_1 + 1} = H_1 \tag{8}$$

Similarly, for points $(0, G_2, 1)^T$ and $(0, H_2, 1)^T$, we can have

$$\frac{w_y G_2}{k'_y G_2 + 1} = H_2 \tag{9}$$

From Eqs. (8) and (9), we can solve w_y and k'_y as

$$\begin{cases} w_y = \dfrac{(G_2 - G_1) H_1 H_2}{(H_2 - H_1) G_1 G_2} \\ k'_y = \dfrac{H_1 G_2 - H_2 G_1}{(H_2 - H_1) G_1 G_2} \end{cases} \tag{10}$$

The matrix $\mathbf{A}_2\mathbf{T}_v$ aligns all the horizontal epipolar lines in the right image to their matching horizontal epipolar lines in the left image.

2.3 Keystone Effect Correction

After the alignment step as described early, matching epipolar lines are horizontal and are on the same scanline. However, the spacings between the three epipolar lines used earlier may not be the same due to the projective transformation. This is similar to the keystone effect in projector projections. To remove the keystone effect, i.e., to make the spacings between the horizontal epipolar lines equal, we develop the following new method for our rectification purpose for reducing transformation distortions. In Figure 2, different spacings $|H_1|$ and $|H_2|$ between neighboring epipolar lines are to be transformed to the same spacing S.

With the law of sine, the relationships between some quantities of the triangles $\triangle$AA$'$O and that of $\triangle$DD$'$O as shown in Figure 2 can be written as:

$$\frac{\sin\alpha_1}{S} = \frac{\sin\beta_1}{H_1} \quad \text{and} \quad \frac{\sin(\pi - \alpha_2)}{S} = \frac{\sin\beta_2}{H_2} \tag{11}$$

which leads to

$$\frac{\sin\alpha_1}{\sin(\pi - \alpha_2)} = \frac{H_2 \sin\beta_1}{H_1 \sin\beta_2} \tag{12}$$

From this equation, we are to find the angle θ as shown in Figure 2 and then the length S. With $\beta_1 = \pi - \alpha_1 - \theta$ and $\beta_2 = \alpha_2 - \theta$, we have

$$\frac{\sin\alpha_1}{\sin(\pi - \alpha_2)} = \frac{H_2 \sin(\pi - \alpha_1 - \theta)}{H_1 \sin(\alpha_2 - \theta)} \tag{13}$$

and with the angle sum and angle difference formulae, one has

$$\frac{H_1 \sin\alpha_1}{H_2 \sin\alpha_2} = \frac{\sin\alpha_1 \cos\theta + \cos\alpha_1 \sin\theta}{\sin\alpha_2 \cos\theta - \cos\alpha_2 \sin\theta} \tag{14}$$

The solution for θ can be obtained from Eq. (14) and equation $\sin^2\theta + \cos^2\theta = 1$ as the following:

$$\theta = \pm \arcsin\sqrt{1/(1+g^2)} \tag{15}$$

with

$$g = \frac{H_1 \sin\alpha_1 \cos\alpha_2 + H_2 \cos\alpha_1 \sin\alpha_2}{H_1 \sin\alpha_1 \sin\alpha_2 - H_2 \sin\alpha_1 \sin\alpha_2}. \tag{16}$$

There are two solutions for θ. We choose the one which satisfies Eq. (14). The values of α_1 and α_2 can be obtained from f, H_1 and H_2. With uncalibrated images, f is set to 1. From the obtained θ, we can calculate β_1 and then the length S can be calculated as $S = H_1 \sin\alpha_1 / \sin\beta_1$.

The keystone correction matrix can be obtained using the same procedure as used when calculating $\mathbf{A}_2$ but with $G_1 = S$ and $G_2 = -S$. Given that there is only a projective transformation without scaling for keystone effect correction, one can have a simpler matrix

$$\begin{pmatrix} 1 & 0 & 0 \\ 0 & 1 & 0 \\ 0 & k' & 1 \end{pmatrix} \tag{17}$$

with k' as the unknown. The transformed point of $(0, H_1, 1)^T$ becomes

$$\begin{pmatrix} 1 & 0 & 0 \\ 0 & 1 & 0 \\ 0 & k' & 1 \end{pmatrix} \begin{pmatrix} 0 \\ H_1 \\ 1 \end{pmatrix} = \begin{pmatrix} 0 \\ H_1 \\ k'H_1 + 1 \end{pmatrix} \sim \begin{pmatrix} 0 \\ \frac{H_1}{k'H_1 + 1} \\ 1 \end{pmatrix} \tag{18}$$

This point matches $(0, S, 1)^T$. Hence we have

$$\frac{H_1}{k'H_1 + 1} = S \qquad \text{i.e.} \qquad k' = \frac{H_1 - S}{H_1 S} \tag{19}$$

Here we denote the newly obtained matrix as $\mathbf{H}$ for keystone effect correction which will be applied to both left and right

images. That is

$$\mathbf{H} = \begin{pmatrix} 1 & 0 & 0 \\ 0 & 1 & 0 \\ 0 & \frac{H_1 - S}{H_1 S} & 1 \end{pmatrix} \tag{20}$$

2.4 Deskewing Images

The rectified images after keystone effect correction can be further processed so that two orthogonal vectors in an original image are close to orthogonal in the rectified image. The two orthogonal vectors in the original image can go through the image center, one horizontal and one vertical. Assuming the two transformed vectors after keystone effect correction, i.e., after applying $\mathbf{HP}_1$ to the original orthogonal vectors, are $m = (u_1, v_1, 0)^T$ and $n = (u_2, v_2, 0)^T$, with a skew matrix

$$\mathbf{S}_1 = \begin{pmatrix} 1 & s_1 & 0 \\ 0 & 1 & 0 \\ 0 & 0 & 1 \end{pmatrix}, \tag{21}$$

we wish to make the two transformed vectors m and n after applying $\mathbf{S}_1$ orthogonal to each other, i.e., their dot product is zero: $\langle \mathbf{S}_1 m, \mathbf{S}_1 n \rangle = 0$. This gives an equation with variable s_1:

$$v_1 v_2 s_1^2 + (u_1 v_2 + u_2 v_1) s_1 + u_1 u_2 + v_1 v_2 = 0 \tag{22}$$

and it can be solved with two solutions. The one with the smallest absolute value is taken as s_1. The matrix for the right image $\mathbf{S}_2$ can be obtained similarly, using $\mathbf{HA}_2\mathbf{T}_v\mathbf{P}_2$ instead of $\mathbf{HP}_1$.

2.5 Reducing Image Translation

The rectified images obtained by applying the transformation matrix $\mathbf{S}_1\mathbf{HP}_1$ for the left image and $\mathbf{S}_2\mathbf{HA}_2\mathbf{T}_v\mathbf{P}_2$ for the right image are almost always different from the original images. Our intention is to minimize the image difference before and after the rectification process. An image translation can be carried out by using the sum of the position differences for the four corners of the rectified and the original images.

The vertical shift should have the same value for both the left and right rectified images, i.e., $v_1' = v_2'$. They are obtained by calculating the average vertical differences of both the four corners in the left image and the four corners in the right image, i.e., totaling of eight corners, before and after applying transformations $\mathbf{S}_1\mathbf{HP}_1$ and $\mathbf{S}_2\mathbf{HA}_2\mathbf{T}_v\mathbf{P}_2$.

The horizontal shifts u_1' and u_2' for the left and right images can be different and will be obtained independently for each image. u_1' is obtained by calculating the average horizontal differences of the four corners in the left image before and after applying transformations $\mathbf{S}_1\mathbf{HP}_1$. Similarly u_2' is obtained for the right image using transformation $\mathbf{S}_2\mathbf{HA}_2\mathbf{T}_v\mathbf{P}_2$. The transformation matrix for the shifts are

$$\mathbf{T}_1 = \begin{pmatrix} 1 & 0 & -u_1' \\ 0 & 1 & -v_1' \\ 0 & 0 & 1 \end{pmatrix} \quad \text{and} \quad \mathbf{T}_2 = \begin{pmatrix} 1 & 0 & -u_2' \\ 0 & 1 & -v_2' \\ 0 & 0 & 1 \end{pmatrix} \tag{23}$$

2.6 Algorithm Steps

The combined transformations to achieve the final image rectifications are through the use of $\mathbf{T}_1\mathbf{S}_1\mathbf{HP}_1$ and $\mathbf{T}_2\mathbf{S}_2\mathbf{HA}_2\mathbf{T}_v\mathbf{P}_2$ for the left and right images respectively. If we put the transformations in groups, they become:

$$\begin{array}{lcccc} \textit{for left image:} & \mathbf{T}_1\mathbf{S}_1 & \mathbf{H} & & \mathbf{K}_1\mathbf{R}_1\mathbf{T} \\ \textit{for right image:} & \underbrace{\mathbf{T}_2\mathbf{S}_2}_{\uparrow\ ④} & \underbrace{\mathbf{H}}_{\uparrow\ ③} & \underbrace{\mathbf{A}_2\mathbf{T}_v}_{\uparrow\ ②} & \underbrace{\mathbf{K}_2\mathbf{R}_2\mathbf{T}}_{\uparrow\ ①} \end{array}$$

The transformations in group ① project the epipoles in the two images to infinity and therefore all the epipolar lines become horizontal. Transformations in group ② for the right image align the matching epipolar lines between two images. The $\mathbf{H}$ matrix in group ③ corrects the keystone effect so that the spacings between epipolar lines become regular or the same. The transformations in group ④ deskew and shift transformed images to minimize distortion. The steps of our algorithm for stereo image rectification are the following:

1. Obtain or read in the fundamental matrix between two views.
2. Uncalibrated stereo image rectification:
   (a) Calculate the epipoles on the two images from the $\mathbf{F}_{12}$ matrix.
   (b) Obtain the transformation matrices $\mathbf{P}_1$ and $\mathbf{P}_2$ for the left and right images using the method described in Section 2.1.
   (c) Obtain alignment transformation $\mathbf{A}_2\mathbf{T}_v$ for the right image.
   (d) Obtain keystone correction transformation $\mathbf{H}$ for both images.
   (e) Obtain the deskewing matrices $\mathbf{S}_1$ and $\mathbf{S}_2$, and obtain the translation matrices $\mathbf{T}_1$ and $\mathbf{T}_2$.
   (f) Apply the two transformation matrices $\mathbf{T}_1\mathbf{S}_1\mathbf{HP}_1$ and $\mathbf{T}_2\mathbf{S}_2\mathbf{HA}_2\mathbf{T}_v\mathbf{P}_2$ to the left and right images respectively and apply resamplings to obtain the rectified images.

3. EXPERIMENTAL RESULTS

This section shows some of the stereo image rectification results obtained using our new method described in previous sections and also gives some comparison results. A variety of real images have been tested. The fundamental matrix for each pair of images can be obtained using the method proposed in [18]. After we have obtained the fundamental matrix for a pair of images, we can then carry out the rectification process using our rectification algorithm. When resampling the input images for rectification, bilinear interpolation can be used.

Figure 3 shows the results for the main steps of our rectification process. Figure 3(a,b) show the epipolar lines overlaid on the original stereo images. Figure 3(c,d) show the epipolar lines transformed into horizontal lines. Note that the matching epipolar lines are not yet aligned to each other. Figure 3(e,f) show that the matching epipolar lines are aligned between the left and right images. Figure 3(g,h) are the final rectification results after correcting keystone effect, deskewing, and shifts. Figure 4 shows another example of our rectification results. Figure 4(a,b) show the epipolar lines overlaid on the original stereo images, and Figure 4(c,d) are the final rectification results.

For majority of the cases, the keystone effects are minimum especially when the epipoles are further away from the image centers. Figure 5 shows an example of keystone effect correction for the right image of a stereo pair. Figure 5(a) shows the epipolar lines with different spacings, with larger spacings on the upper part and smaller spacings on the lower part of the image, while Figure 5(b) shows epipolar lines with the same spacing after keystone effect correction for the same image.

In [11], Mallon and Whelan compared their method with two other popular methods from the literature, Hartley's [6]

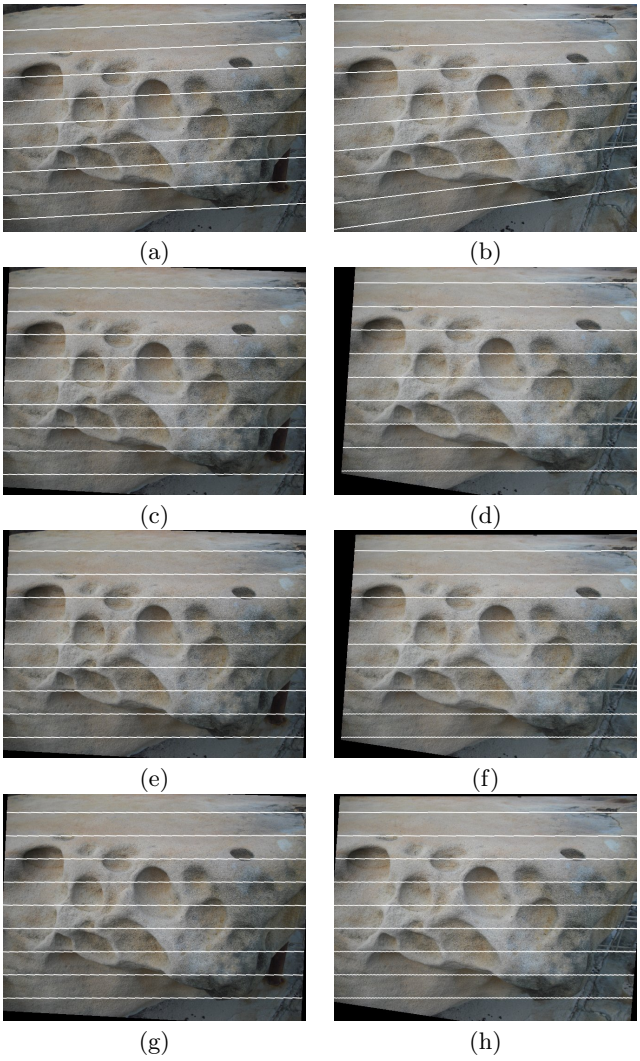

Figure 3: Rectification results for the main steps of our algorithm. (a,b) Epipolar lines overlaid on the original stereo images; (c,d) Epipolar lines transformed into horizontal lines; (e,f) Matching epipolar lines aligned between the left and right images; (g,h) Final rectification results after correcting keystone effect, deskewing, and shifts.

and Loop and Zhang's [10]. Mallon and Whelan's results showed that their method gives a much improved performance than the other two methods. Our experimental results also confirmed that the results of [11] are better than that of [6] and [10]. Because of this and the limitation of space, in this paper we just show the results of our method and that of Mallon and Whelan's method which is currently the state-of-the-art. Both our method and Mallon and Whelan's method use the same input for rectification, i.e., only the fundamental matrix information. Figure 6 shows the comparison results between ours and that of Mallon and Whelan's using the same set of fundamental matrices on the 'Slate' dataset. The 'Slate' dataset is an indoor office scene. It can be seen that our method produces smaller areas of black pixels, i.e., more usable pixel areas in the rectified images. The method in [11] does not have all the distortion

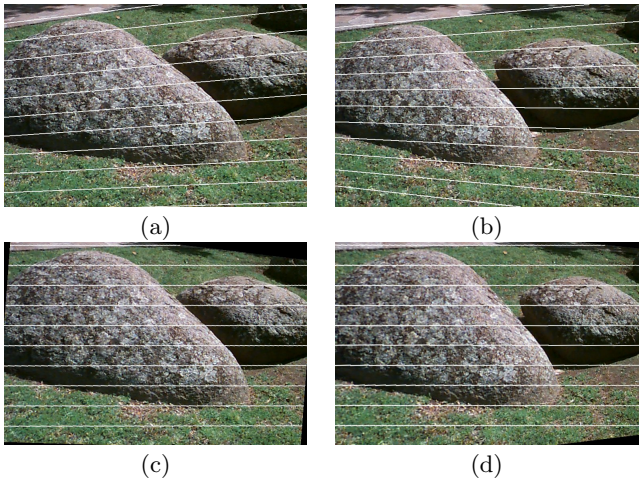

Figure 4: Another example of our rectification results. (a,b) Epipolar lines overlaid on the original stereo images. (c,d) Final rectification results.

reduction steps as in our method.

In terms of running times, our rectification process is very fast, taking about 81 ms for a 640×480 pixel image on a Linux PC with a 3.00GHz Intel Core2Duo CPU using the C language. The majority of the CPU time was on the actual image resampling process which takes about 76 ms. The process for obtaining the rectification matrices only takes about 4.7 ms.

4. CONCLUSIONS

In this paper, a new closed-form method for automatically rectifying uncalibrated stereo images has been presented. The transformation matrices applied to the original images are constructed just based on the epipolar geometries between an image pair, i.e. only using the fundamental matrix. There is no iterative parameter optimization process in our methods. That is our method is in closed-form and with just the fundamental matrix. Real images have been tested and the results validate our new method. Comparison with the state-of-the-art method shows that our method produces better rectification results. Future work should include more quantitative evaluations of different rectification methods.

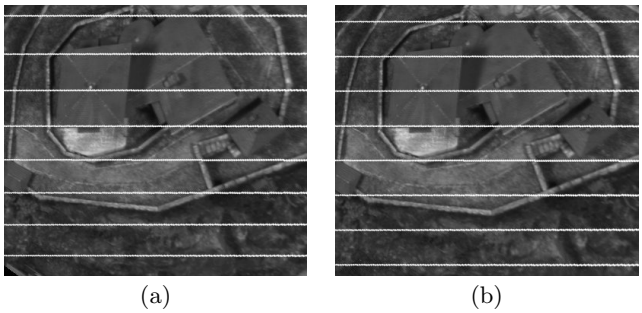

Figure 5: An example showing the keystone effect correction. (a) Epipolar lines with different spacings. (b) Epipolar lines with the same spacing.

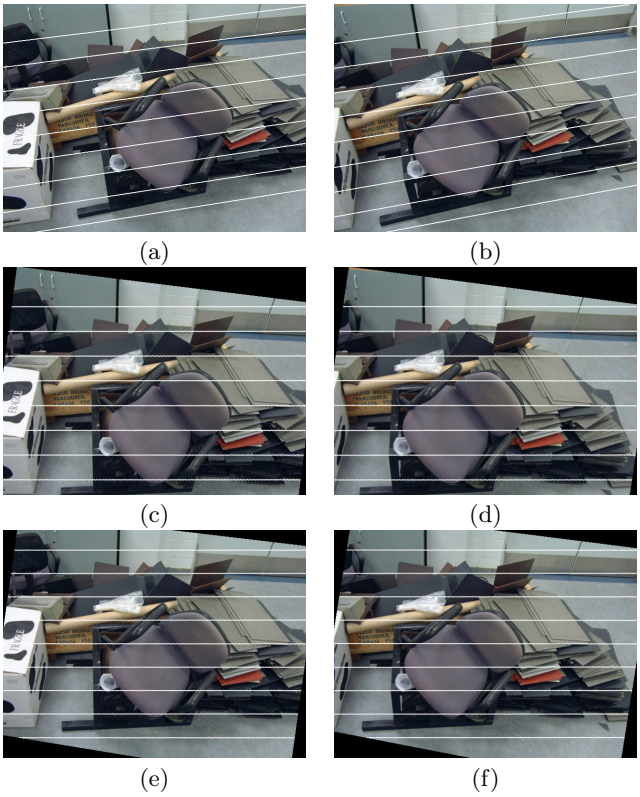

Figure 6: Rectification results of ours and Mallon and Whelan's on the 'Slate' dataset. (a,b) Epipolar lines overlaid on the original stereo images. (c,d) Results using Mallon and Whelan's method. (e,f) Results using our method.

5. ONLINE DEMO

An online web demo for stereo image rectification using our method is available at:

`vision-cdc.csiro.au/rectify2v`

6. ACKNOWLEDGEMENTS

The author thanks Xiao Tan of CSIRO and the anonymous reviewers for their comments and suggestions. The author is also grateful to Dr John Mallon from Dublin City University for sample MATLAB codes described in [11]. The images and related data in Figure 6 are from Dr Mallon. This research was partially supported by the CSIRO's Transformational Biology Capability Platform.

7. REFERENCES

[1] N. Ayache and C. Hansen. Rectification of images for binocular and trinocular stereovision. In *Proceedings of International Conference on Pattern Recognition*, volume 1, pages 11–16, Rome, Italy, November 1988.

[2] Z. Chen, C. Wu, and H. T. Tsui. A new image rectification algorithm. *Pattern Recognition Letters*, 24(1-3):251–260, January 2003.

[3] A. Fusiello and L. Irsara. Quasi-Euclidean epipolar rectification of uncalibrated images. *Machine Vision Applications*, 22(4):663–670, July 2011.

[4] A. Fusiello, E. Trucco, and A. Verri. A compact algorithm for rectification of stereo pairs. *Machine Vision Applications*, 12(1):16–22, July 2000.

[5] J. Gluckman and S. K. Nayar. Rectifying transformations that minimize resampling effects. In *Proceedings of Computer Vision and Pattern Recognition*, volume 1, pages 111–117, 2001.

[6] R. Hartley. Theory and practice of projective rectification. *International Journal of Computer Vision*, 35(2):115–127, November 1999.

[7] F. Isgro and E. Trucco. Projective rectification without epipolar geometry. In *IEEE Conference on Computer Vision and Pattern Recognition*, volume 1, pages 1094–1099, 23-25 June 1999.

[8] K. Jawed, J. Morris, T. Khan, and G. Gimel'farb. Real time rectification for stereo correspondence. In *International Conference on Computational Science and Engineering*, volume 2, pages 277–284, 2009.

[9] S. Kumar, C. Micheloni, C. Piciarelli, and G. L. Foresti. Stereo rectification of uncalibrated and heterogeneous images. *Pattern Recognition Letters*, 31(11):1445–1452, August 2010.

[10] C. Loop and Z. Zhang. Computing rectifying homographies for stereo vision. Technical Report MSR-TR-99-21, Microsoft Research, 8 April 1999.

[11] J. Mallon and P. F. Whelan. Projective rectification from the fundamental matrix. *Image and Vision Computing*, 23(7):643–650, July 2005.

[12] P. Monasse, J.-M. Morel, and Z. Tang. Three-step image rectification. In *Proceedings of the British Machine Vision Conference*, pages 89.1–89.10. BMVA Press, 2010.

[13] D. Oram. Rectification for any epipolar geometry. In *Proceedings of British Machine Vision Conference*, pages 653–662, 2001.

[14] M. Pollefeys, R. Koch, and L. Van Gool. A simple and efficient rectification method for general motion. In *Proceedings of International Conference on Computer Vision*, volume 1, pages 496–501, Corfu, Greece, 20-25 September 1999.

[15] L. Robert, C. Zeller, O. Faugeras, and M. Hebert. Applications of non-metric vision to some visually guided robotics tasks. Technical Report 2584, INRIA, June 1995.

[16] S. Roy, J. Meunier, and I. J. Cox. Cylindrical rectification to minimize epipolar distortion. In *Proceedings of Computer Vision and Pattern Recognition*, pages 393–399, Puerto Rico, June 1997.

[17] C. Sun. Uncalibrated three-view image rectification. *Image and Vision Computing*, 21(3):259–269, March 2003.

[18] Z. Zhang and C. Loop. Estimating the fundamental matrix by transforming image points in projective space. *Computer Vision and Image Understanding*, 82(2):174–180, May 2001.